



HAL
open science

ARACHNIS: Analysis of Robots Actuated by Cables with Handy and Neat Interface Software

Ana Lucia Cruz Ruiz, Stéphane Caro, Philippe Cardou, François Guay

► **To cite this version:**

Ana Lucia Cruz Ruiz, Stéphane Caro, Philippe Cardou, François Guay. ARACHNIS: Analysis of Robots Actuated by Cables with Handy and Neat Interface Software. The Second International Conference on Cable-Driven Parallel Robots (CableCon 2014), Aug 2014, Duisburg, Germany. hal-01941633

HAL Id: hal-01941633

<https://hal.science/hal-01941633>

Submitted on 1 Dec 2018

HAL is a multi-disciplinary open access archive for the deposit and dissemination of scientific research documents, whether they are published or not. The documents may come from teaching and research institutions in France or abroad, or from public or private research centers.

L'archive ouverte pluridisciplinaire **HAL**, est destinée au dépôt et à la diffusion de documents scientifiques de niveau recherche, publiés ou non, émanant des établissements d'enseignement et de recherche français ou étrangers, des laboratoires publics ou privés.

ARACHNIS: Analysis of Robots Actuated by Cables with Handy and Neat Interface Software

Ana Lucia Cruz Ruiz¹, Stéphane Caro², Philippe Cardou³, and François Guay³

¹ IRCCyN, École Centrale de Nantes, 1 rue de la Noë, 44321, Nantes, France, e-mail: analu.610@gmail.com

² CNRS-IRCCyN, 1 rue de la Noë, 44321, Nantes, France, e-mail: stephane.caro@irccyn.ec-nantes.fr

³ Laboratoire de robotique, Département de génie mécanique, Université Laval, Quebec City, QC, Canada. e-mail: pcardou@gmc.ulaval.ca, francois.guay.2@ulaval.ca

Abstract. This paper presents ARACHNIS, a graphical user interface for the analysis and parametric design of Cable Driven Parallel Robots (CDPRs). ARACHNIS takes as inputs the design parameters of the robot, the task specifications, and returns a visualisation of the CDPR Wrench Feasible Workspace (WFW) and Interference-Free Constant Orientation Workspace (IFCOW). The WFW is traced from the capacity margin, a measure of the robustness of the equilibrium of the robot. Interferences between the moving parts of a CDPR are also determined by an existing technique for tracing the interference-free workspace of such robots. Finally, the WFW and the IFCOW of a planar cable-driven parallel robot and of a spatial cable-driven parallel robot are plotted in order to demonstrate the potential of ARACHNIS.

Key words: workspace, wrench-feasible workspace, interference, graphical user interface, capacity margin, static equilibrium, cable-driven robot, wire-driven robot

1 Introduction

Cable-Driven Parallel Robots (CDPRs) may be seen as Gough-Stewart platforms in which the prismatic actuators are replaced with cables. Hence, the cables are connected between the moving platform and fixed eyelets. The platform moves around by increasing or decreasing the lengths of the different cables in concert while preventing any cable from becoming slack [11]. This architecture allows for marked advantages over conventional robots, such as the possibility of a larger workspace and higher accelerations, thanks to lighter mechanical components. CPDRs also suffer from important drawbacks, however. First, there is the possibility of interferences among the cables or between a cable and the moving platform. Furthermore, the non-rigid nature of the CPDR links further restrict its workspace, and requires a rigorous study of its force transmission characteristics.

Nevertheless, CDPRs have been used, often with success, in many areas such as robotic cranes, cable-driven cameras, medicine, automatic painting and rescue operations, to name but a few. The reader is referred to a recent literature survey on the topic [4] for a more thorough account of these applications. These CDPRs

and others were developed independently, in most cases, meaning that their designers usually started the analysis and design process development “from scratch”. As CDPRs become more popular, there is an obvious need to automate their design and analysis, to accelerate their development and to provide a common working ground to the engineers involved.

To partly answer this need, we propose the graphical user interface ARACHNIS, or Analysis of Robots Actuated by Cables with Handy and Neat Interface Software. In short, ARACHNIS is dedicated to the parameter-based analysis and design of CDPRs. It allows the designer to enter the design parameters of the robot, to specify the task that the robot should perform in terms of force and moment ranges, and to assess the performance of the robot through the visualization of its Wrench-Feasible Workspace (WFW) [3, 5] and its Interference-Free Constant Orientation Workspace (IFCOW) [8]. ARACHNIS seems to be similar in its functions to a previously developed interface named WireCenter [10]. From the little information we could gather on WireCenter, it seems that the two interfaces differ mainly in that WireCenter allows to trace the wrench-closure workspace (WCW), while ARACHNIS allows to trace the WFW.

This workspace was chosen to analyze the static-equilibrium of the robot because it applies to a wider range of tasks than the WCW [6] or the Static Workspace (SW) [12]. In fact, the WCW and the SW can be shown to be special cases of the WFW. To the knowledge of the author, two methods have been reported to trace the WFW of a spatial parallel robot driven by m cables. Both of these methods are purely numerical, since, as was pointed out in [2], computing symbolic expressions of the WFW-boundaries is too complex to be practical in the general case. This spurred other researchers to simply use a brute-force method [1] to trace the WFW as a cloud of points. Others resorted to interval arithmetics to trace the WFW as a set of boxes that are either completely inside the workspace or not completely outside of it [5]. Both of these methods are relatively slow and generally yield poor renderings of the workspace boundary. In ARACHNIS, we resort to an alternative method that was recently proposed by the authors [7], and which, if far from perfect, appears to be somewhat faster and to yield smoother estimates of the WFW than the two existing ones. The IFCOW, on the other hand, is determined according to the method proposed in [9].

The paper is organized as follows: Section 2 describes the kinetostatic model of a cable-driven parallel mechanism. Section 3 introduces the capacity margin as a measure of the robustness of CDPR equilibrium. Section 4 explains how the capacity margin is used to trace the WFW. Section 5 presents the polygons of the IFCOW where interferences occur between the cables and the moving platform. Section 6 describes the ARACHNIS interface. A planar cable-driven parallel mechanism and a spatial cable-driven parallel mechanism are studied in Secs. 7 and 8, respectively. Finally, we present our conclusions and future work in Sec. 9.

2 Kinetostatic Model of a Cable-Driven Parallel Robot

Formally, a cable-driven parallel robot consists of a moving platform connected to a fixed base by a set of m cables acting in parallel. The winding and unwinding of these cables on fixed spools controls the platform motion in space.

To mathematically model this mechanism, let us attach frame \mathcal{P} to the moving platform, and frame \mathcal{F} to the fixed frame, as shown in Fig. 1. The origins of these frames are P and O , respectively. The platform pose may thus be represented by the vector \mathbf{p} pointing from O to P , and by the rotation matrix \mathbf{Q} rotating \mathcal{F} onto \mathcal{P} .

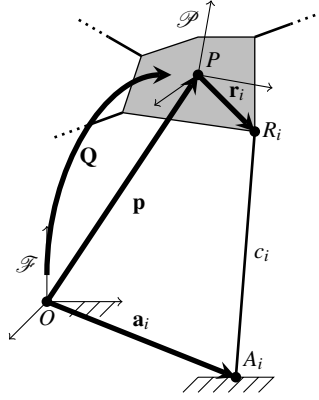


Fig. 1 The kinetostatic model of a cable-driven parallel mechanism

The i^{th} cable is modeled as a straight-line segment from the attachment point onto the moving platform, R_i , to the attachment point onto the fixed frame, A_i . The positions of these attachment points are respectively given by \mathbf{r}_i , expressed in frame \mathcal{P} , and \mathbf{a}_i , expressed in frame \mathcal{F} . The i^{th} cable may thus be represented by the vector

$$\mathbf{c}_i \equiv \mathbf{a}_i - \mathbf{p} - \mathbf{Q}\mathbf{r}_i, \quad (1)$$

and the corresponding cable length is

$$c_i \equiv \|\mathbf{c}_i\|_2, \quad i = 1, \dots, m. \quad (2)$$

Let us now assume that external forces are applied on the moving platform. These forces are equivalent to the resultant force-moment system $\mathbf{w}_e \equiv [\mathbf{f}_e^T (1/r)\mathbf{n}_e^T]^T$, the force $\mathbf{f}_e \in \mathbb{R}^3$ being applied at P , the moment being $\mathbf{n}_e \in \mathbb{R}^3$, and r being a positive length used to render \mathbf{w}_e dimensionally homogeneous. Here, we define this length quite arbitrarily as $r^2 = (1/m)\sum_{i=1}^m \|\mathbf{r}_i\|_2^2$. For the moving platform to remain in equilibrium, there must be a combination of cable tensions $\mathbf{t} \equiv [t_1 \dots t_m]^T$ that balances the system of external forces. By the application of the Newton-Euler

equations to the moving platform, we obtain

$$\mathbf{W}\mathbf{t} + \mathbf{w}_e = \mathbf{0}_6, \quad (3)$$

where $\mathbf{0}_6$ is the six-dimensional null vector and \mathbf{W} is the Jacobian matrix of the mechanism at this particular pose. This matrix may be computed as

$$\mathbf{W} = \begin{bmatrix} \mathbf{c}_1/c_1 & \cdots & \mathbf{c}_m/c_m \\ (\mathbf{Q}\mathbf{r}_1) \times \mathbf{c}_1/(rc_1) & \cdots & (\mathbf{Q}\mathbf{r}_m) \times \mathbf{c}_m/(rc_m) \end{bmatrix}. \quad (4)$$

To this standard kinetostatic model of a cable-driven parallel robot, let us add limits to the involved forces and moments. Indeed, for a given application, we may safely assume that the designer of a cable-driven parallel mechanism can define a set of external force-moment systems \mathbf{w}_e that can be applied on the mobile platform. We further assume that this set is a box \mathcal{W}_e in \mathbb{R}^6 . For reasons that will later become apparent, let us give the vertex representation of this box, namely,

$$\mathcal{W}_e = \{\mathbf{w}_e \in \mathbb{R}^6 : \mathbf{w}_e = \sum_{j=1}^n \alpha_j \mathbf{w}_{e,j}, \sum_{j=1}^n \alpha_j = 1, \alpha_j \geq 0, j = 1, \dots, n\}, \quad (5)$$

where $\mathbf{w}_{e,j}$, $j = 1, \dots, 64$ are the vertices of \mathcal{W}_e .

The cable tensions t_i , $i = 1, \dots, m$, are also limited by the load capacities of the motors and by the strengths of the cables and spool transmission elements. From the components he/she selected, the designer should thus be able to assess the lower and upper tension bounds, respectively $\underline{\mathbf{t}}$ and $\bar{\mathbf{t}}$. Formally, these define the m -dimensional box of feasible tensions

$$\mathcal{T} = \{\mathbf{t} \in \mathbb{R}^m : \underline{\mathbf{t}} \leq \mathbf{t} \leq \bar{\mathbf{t}}\}. \quad (6)$$

3 The Capacity Margin as a Measure of the Robustness of Equilibrium

According to the model of a cable-driven parallel robot presented above, the moving platform is in equilibrium for every possible external force-moment system \mathbf{w}_e if and only if, in every case, the Newton-Euler equilibrium, eq. (3), can be satisfied by a set of feasible cable tensions \mathbf{t} . Such a pose of “complete” equilibrium of the moving platform is often called a “feasible pose” in the scientific literature. The set of all feasible poses is called the “wrench-feasible workspace” (WFW), and is formally expressed in Definition 1.

Definition 1. The wrench-feasible workspace \mathcal{F} is defined as

$$\mathcal{F} = \{(\mathbf{p}, \mathbf{Q}) \in \mathbb{R}^3 \times SO(3) : \forall \mathbf{w}_e \in \mathcal{W}_e, \exists \mathbf{t} \in \mathcal{T}, \mathbf{W}\mathbf{t} + \mathbf{w}_e = \mathbf{0}_6\}, \quad (7)$$

where $SO(3)$ is the group of proper rotation matrices, \mathcal{W}_e is defined in eq. (5), \mathcal{T} is defined in eq. (6), and \mathbf{W} is defined in eq. (4).

The capacity margin was recently introduced by the same authors in [7] under the name *minimum degree of constraint satisfaction*. We believe that the name *capacity margin* describes better this index, if only for the sake of brevity, but for other reasons that will be made apparent from its definition.

This definition stems from the geometric interpretation of the wrench-feasible workspace, which is represented in Fig. 2. The two sets involved in the definition of \mathcal{F} , \mathcal{W}_e and \mathcal{T} , live in different spaces and have different numbers of dimensions. In this paper, we assume the number of dimensions of \mathcal{W}_e to be six, although the proposed method applies equally well to lower dimensional cases. The number of cables m corresponds to the number of dimensions of \mathcal{T} . For the sake of illustration, the dimensions of \mathcal{W}_e and \mathcal{T} in Fig. 2 were chosen to be two and three, respectively. The two sets are connected by eq. (3), by which the tensions, \mathbf{t} , are linearly mapped onto the wrench space via the transformation $-\mathbf{W}$. Hence, the box \mathcal{T} of feasible tensions becomes the zonotope \mathcal{W}_t in the wrench space.

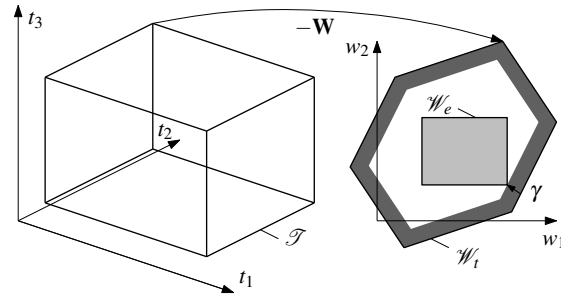


Fig. 2 An analog geometric representation of the capacity margin γ

From the definition of the wrench-feasible workspace, this zonotope should include the set \mathcal{W}_e of external wrenches. Indeed, for an external wrench \mathbf{w}_e to be sustained by the moving platform, there must exist a set of tensions in \mathcal{T} such that $\mathbf{w}_e = -\mathbf{W}\mathbf{t}$. Geometrically, this means that the point \mathbf{w}_e should be contained in \mathcal{W}_t . Therefore, for any external wrench to be sustained, we should have

$$\mathcal{W}_e \subseteq \mathcal{W}_t, \quad (8)$$

which gives us a necessary and sufficient condition for a pose (\mathbf{p}, \mathbf{Q}) to be wrench-feasible.

This binary condition does not tell us how far is a feasible pose from being unfeasible. Such a question is important to the designer, as an answer would indicate the robustness of the equilibrium. This is precisely what the capacity margin represents.

In Fig. 2, the capacity margin is geometrically represented by γ , the signed width of the margin between the boundary of \mathcal{W}_t and \mathcal{W}_e . This width is taken positive when

the margin is inside \mathcal{W}_i , and negative when it is outside. It may thus be seen as the degree of inclusion of \mathcal{W}_e within \mathcal{W}_i .

Mathematically, we compute γ as follows:

1. Compute the facet representation of \mathcal{W}_i using the hyperplane shifting method [3]. We thus obtain \mathbf{a}_l and b_l , $l = 1, \dots, p$ in the equation $\mathcal{W}_i = \{\mathbf{w} \in \mathbb{R}^6 : \mathbf{a}_l^T \mathbf{w} \leq b_l, l = 1, \dots, p\}$.
2. Compute the coordinate $\gamma_{j,l}$ of each vertex $\mathbf{w}_{e,j}$ of \mathcal{W}_e with each facet (\mathbf{a}_l, b_l) of \mathcal{W}_i . This coordinate is taken from the facet in its normal direction \mathbf{a}_l , which gives $\gamma_{j,l} = (b_l - \mathbf{w}_{e,j}^T \mathbf{a}_l) / \|\mathbf{a}_l\|_2$, $j = 1, \dots, n$, $l = 1, \dots, p$.
3. Keep the minimum of all coordinates as a worst case scenario:

$$\gamma = \min_{j=1, \dots, n} \min_{l=1, \dots, p} \gamma_{j,l}.$$

4 Tracing the Wrench-Feasible Workspace Using the Capacity Margin

The capacity margin γ indicates the *degree of inclusion* of the set \mathcal{W}_e of external wrenches into the set \mathcal{W}_i of feasible wrenches. γ is a greater *positive* scalar as \mathcal{W}_e is further inside \mathcal{W}_i opposed to being a greater *negative* scalar as at least a part of \mathcal{W}_e is further outside \mathcal{W}_i . Consequently, γ is zero when $\mathcal{W}_e \subseteq \mathcal{W}_i$ and a point of \mathcal{W}_e is on the boundary of \mathcal{W}_i . From definition 1, this latter case corresponds to a pose that is on the limit of feasibility. Hence, the boundary of the wrench-feasible workspace may simply be expressed as

$$\gamma(\mathbf{p}, \mathbf{Q}) = 0. \quad (9)$$

In this paper, we use this fact to trace the boundary of the wrench-feasible workspace as the zero *isosurface* or *isocontour* of the capacity margin. To compute the zero isocontour of a function, one first needs to evaluate it at a grid of points covering its domain. The next step consists in interpolating the between adjacent points of the grid in search of roots of the function. This process is readily implemented in virtually all scientific computation packages. In `Matlab`, for instance, the functions `isosurface` and `contour` can be used to trace the isosurface and isocontour of a function, respectively. In `Maple`, the analogous functions are `implicitplot3d` and `implicitplot`.

5 Tracing the Interference Polygons

The wrench-feasible workspace alone is not sufficient to design a cable-driven parallel robot. Interferences between the moving parts must also be considered, either by shear intuition or by systematic analysis. A technique for such analysis of the interference-free workspace was proposed in [9], and was implemented in ARACHNIS. Let us note, however, that the technique only applies to a constant orientation

of the moving platform. Moreover, it is developed under the assumptions that the cables are line segments and that the moving platform is a convex polyhedron represented by its edges.

In [9], it was shown that the region of the Cartesian space where a pair of cables collide is composed of two disjoint polygons in space. Mathematically, the two polygons corresponding to an interference between the i^{th} and j^{th} cables may be expressed as

$$\mathcal{C}_{i,j} = \{\mathbf{p} \in \mathbb{R}^3 : \mathbf{p} = \mathbf{a}_j - \mathbf{Q}\mathbf{r}_i + \alpha(\mathbf{a}_j - \mathbf{a}_i) + \beta\mathbf{Q}(\mathbf{r}_j - \mathbf{r}_i), \alpha, \beta \geq 0\}, \quad (10a)$$

$$\mathcal{C}_{j,i} = \{\mathbf{p} \in \mathbb{R}^3 : \mathbf{p} = \mathbf{a}_i - \mathbf{Q}\mathbf{r}_j + \alpha(\mathbf{a}_i - \mathbf{a}_j) + \beta\mathbf{Q}(\mathbf{r}_i - \mathbf{r}_j), \alpha, \beta \geq 0\}. \quad (10b)$$

Interferences can also occur between a cable and the moving platform. The associated interference regions are computed in [9]. This is done by tracing the interference region between the i^{th} cable and the edge connecting the j^{th} and k^{th} vertices of the polyhedron-shaped moving-platform. Let the positions of these vertices be represented by \mathbf{v}_j and \mathbf{v}_k , respectively, in the mobile frame \mathcal{P} . In this case, the interference region $\mathcal{E}_{i,j,k}$ takes the form of a polygon in space, that is,

$$\mathcal{E}_{i,j,k} = \{\mathbf{p} \in \mathbb{R}^3 : \mathbf{p} = \mathbf{a}_i - \mathbf{Q}\mathbf{r}_i + \nu_j\mathbf{Q}(\mathbf{v}_j - \mathbf{b}_i) + \nu_k\mathbf{Q}(\mathbf{v}_k - \mathbf{b}_i), \\ \nu_j, \nu_k \leq 0, \nu_j + \nu_k \leq -1\}. \quad (11)$$

Notice that the regions $\mathcal{C}_{i,j}$ and $\mathcal{E}_{i,j,k}$ are unbounded in some directions. In ARACHNIS, we assume that the portion of interest of the Cartesian workspace is a box containing all the fixed points $A_i, i = 1, \dots, m$. In the proposed interface, we thus trace the intersections of this box with the interference regions $\mathcal{C}_{i,j}, i, j = 1, \dots, m$, and $\mathcal{E}_{i,j,k}, i = 1, \dots, m, j, k = 1, \dots, q$, where q is the number of vertices of the moving platform.

6 The ARACHNIS Interface

ARACHNIS, or ‘‘Analysis of Robots Actuated by Cables with Handy and Neat Interface Software’’, is a graphical user interface developed in MATLAB to automate the design and the analysis of CDPs. At the conceptual design stage, this tool aids the designer in choosing the design that best meets two requirements: equilibrium throughout the workspace and interference avoidance.

The interface provides the degree to which these requirements are satisfied for a particular design through the generation of the WFW and the IFCOW. As shown in Fig. 3, it is divided into four main areas: Robot Parameters, Robot Posture, Robot Task and Robot Visualization.

The section *Robot Parameters* is dedicated to the specification of the geometry of the platform and base, cable tension limits and cable arrangement. The geometry of the platform is described through the Cartesian coordinates of the cable anchor points

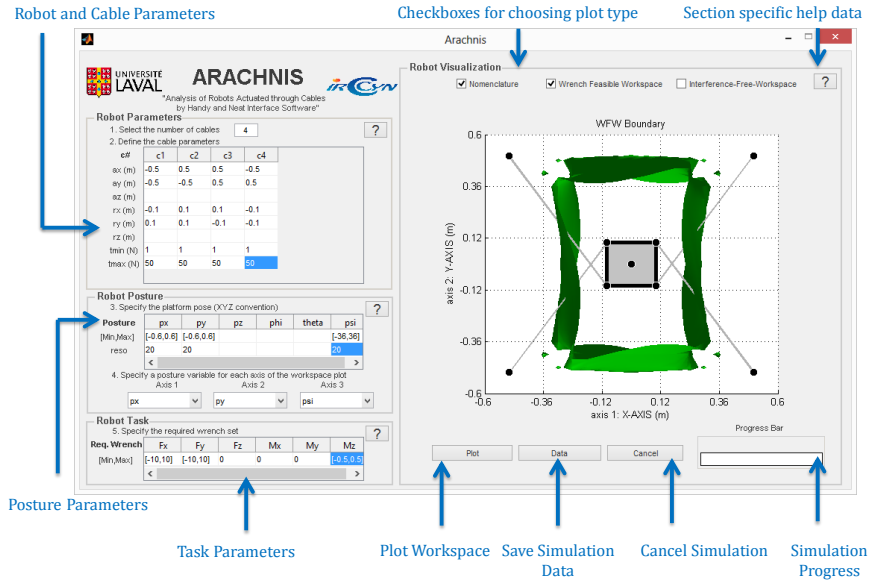


Fig. 3 ARACHNIS and its main features

on the platform (rx , ry and rz) expressed in the platform frame and the geometry of the base is described through the Cartesian coordinates of the cable anchor points on the base (ax , ay and az) expressed in the base frame. The tension limits are specified via the minimum and maximum tensions allowed in each cable.

In the section *Robot Posture*, the poses required from the platform during a specific task are specified through positions and orientations with respect to the X, Y and Z axes (px , py , pz , ϕ , θ , ψ). The angles ϕ , θ and ψ are the Euler angles specifying the attitude of the platform frame with respect to the fixed frame according to the XYZ convention. Fixed positions and orientations are specified by single numbers, while parameters that vary are specified by intervals and resolutions. Each varying parameter is then assigned to a workspace axis through the pop-up menus.

By allowing any combination and assignation of parameters to the workspace axes, ARACHNIS is able to generate any WFW from two to six dimensions. The WFW above three dimensions cannot be traced in three-dimensional space, of course. In such cases, three of the axes are selected to trace the workspace. The poses contained in the WFW are then the poses for which the full range of poses in the remaining axes are wrench-feasible poses.

The section *Robot Task* consists in describing the prescribed robot task by specifying intervals of forces and moments along each dimension (F_x , F_y , F_z , M_x , M_y , M_z). The forces are assumed to be applied at the origin of the moving-platform

frame, but the components of the forces and moments are parallel to the axes of the fixed frame.

The section *Robot Visualization* consists of a graphical area to visualize the CDPR geometry, its WFW and its IFCOW. This information can be hidden or shown by first clicking the corresponding checkboxes and then clicking the *plot* button. This section also contains a *data* button, which generates an Excel spreadsheet containing the information on the interface and the simulation data, a *cancel* button to stop the workspace computation, and a progress bar to indicate the simulation progress. ARACHNIS also contains *Help* buttons and error messages customized for each section to guide the user as he or she inputs the parameters.

7 Case Study 1: A Planar Cable-Driven Parallel Mechanism

This case study demonstrates the capacity of ARACHNIS to generate the wrench feasible workspace (WFW) of planar cable-driven mechanisms. The mechanism under study is the eight-cable robot shown in Fig. 4, which has previously been analyzed in [13]. As in [13], the tension limits were set to 10 N and 1000 N and no external wrench was applied. The *total orientation workspace* in Fig. 4 was computed by displacing the robot in a $1.2 \text{ m} \times 1.2 \text{ m} \times 120^\circ$ grid using a resolution of 80 points per axis.

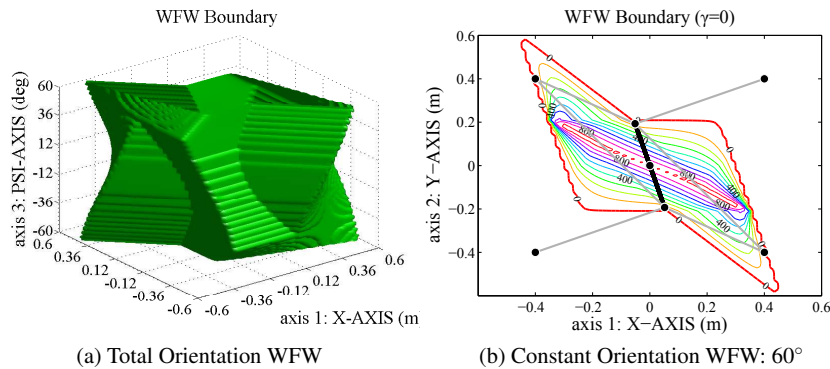


Fig. 4 Wrench Feasible Workspace (WFW) of a planar robot

The green iso-surface corresponding to $\gamma = 0$ represents the frontier of the WFW. Inside this boundary the robot can safely perform the task. We can acquire a more quantitative view of the stability of the robot by slicing the total orientation workspace and generating the *constant orientation workspace* shown in Fig. 4. Each contour in the figure represents a value of γ . Again, the contour where $\gamma = 0$ defines the stability frontier. The higher this value, the greater the robustness of the moving-

platform equilibrium. Notice that these results match those obtained in [13]. Other examples of the workspaces generated by ARACHNIS were done by the same authors in [7], which match the workspaces in ref. [5]. The computation time reported in [5] was 51 s, while that obtained with ARACHNIS was 6 s. This time difference is significant, and cannot be attributed only to the different personal computers that were used in the two studies. Notice that all the simulations were done on a Dell Inspiron 15r laptop (Intel Core i7-3537U 2.50 GHz).

8 Case Study 2: A Spatial Cable-Driven Parallel Mechanism

This case study demonstrates the capacity of ARACHNIS to generate workspaces of spatial cable-driven mechanisms. The mechanism under study is the spatial robot with eight cables displayed in Fig. 5, which has also been previously analyzed in [5]. The tension limits for all cables were set to 1 N and 540 N. The externally applied forces along each dimension varied from -10 N to 10 N, while the moments varied from -0.5 N m to 0.5 N m.

The 5D WFW workspace of this robot was generated by translating it along a $1\text{ m} \times 1\text{ m} \times 1\text{ m}$ grid. At each point on this grid, the robot was rotated around the X and Y axes through orientations ranging from -15° to 15° , while retaining a fixed orientation with respect to the Z -axis. The capacity margin was then evaluated at each of these poses. A set of values γ was thus obtained for every position on a 3D grid. The minimum value from each set was selected and assigned to its corresponding position on the grid. Finally, the values were interpolated, creating the boundary shown Fig. 5. As in the previous section, we computed the 2D slices of this higher dimensional workspace to assess quantitatively the performance of the robot. A slice along the XZ plane is also shown in Fig. 5.

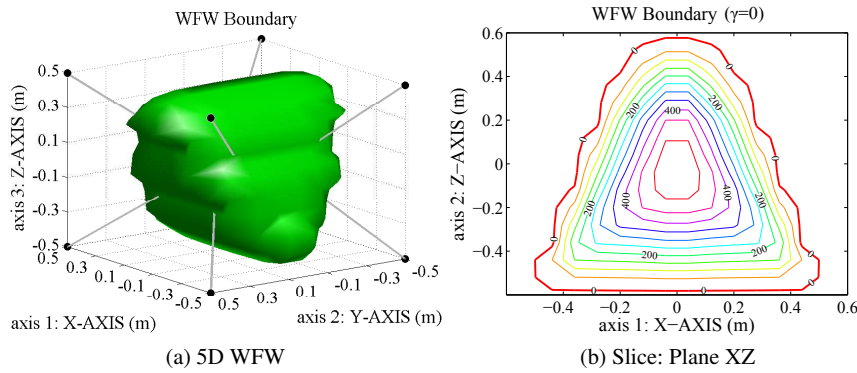


Fig. 5 Wrench Feasible Workspace (WFW) of a spatial robot

These results also match those obtained in [5] by means of interval arithmetics. An argument often made in favor of interval arithmetics is the guarantee of exactness that comes with its results. In the example shown in [5], however, the volume occupied by the uncertainty boxes—boxes that have not been determined to be fully inside or outside the WFW—amounts to 60 % of the total workspace volume. In these conditions, there is no guarantee on the boxes of interest, i.e., those that are close to the boundary of the WFW. Hence, for this example, interval arithmetics offers no more guarantee than any other method. This case study also evidences the computational efficiency of ARACHNIS. The workspace was computed in 225 s, outperforming the algorithm presented in [5] whose computation time was 1567 s. The interference-free constant orientation workspace was also computed through

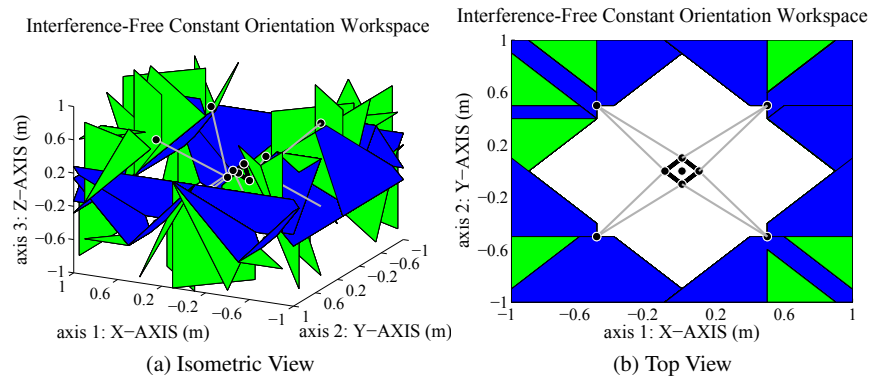


Fig. 6 Interference-Free Constant Orientation Workspace (IFCOW) of a spatial robot

the method described in Sec. 5 and is displayed in Fig. 6. The green polygons symbolize the interference regions between cables, while the blue ones represent the interference regions between a cable and a moving-platform edge. The results show that this robot has an interference free workspace within a box of $1\text{ m} \times 1\text{ m} \times 1\text{ m}$.

9 Conclusions

In this paper, we presented a graphical user interface named ARACHNIS, or Analysis of Robots Actuated by Cables with Handy and Neat Interface Software. ARACHNIS allows the design and analysis of Cable Driven Parallel Robots (CD-PRs). It requires the designer to enter the parameters of the robot, to specify the loads involved in the robot task, and to assess the performance of the robot through the visualization of its Wrench Feasible Workspace (WFW) and its Interference-Free Constant Orientation Workspace (IFCOW). The capacity margin was first defined as a measure of the robustness of the moving-platform equilibrium and was

used to trace the wrench-feasible workspace of the CDPRs. Interferences between the moving parts have also been considered. An existing technique for tracing the interference-free workspace of CDPRs was summarized and implemented in ARACHNIS. The WFW and the IFCOW of a planar cable-driven parallel mechanism and of a spatial cable-driven parallel mechanism have been plotted with ARACHNIS. It turns out that ARACHNIS is very competitive in terms of computation time for tracing the WFW and the IFCOW of CDPRs. The use of the proposed capacity margin to compute the wrench-closure workspace, the static workspace and the dynamic workspace of CDPRs and the conversion of ARACHNIS into a stand-alone interface are the subjects of future work.

References

1. Azizian, K., Cardou, P.: The dimensional synthesis of spatial cable-driven parallel mechanisms. *ASME Journal of Mechanisms and Robotics* **5**(4), 044,502 (2013)
2. Bosscher, P., Riechel, A.T., Ebert-Uphoff, I.: Wrench-feasible workspace generation for cable-driven robots. *IEEE Transactions on Robotics* **22**(5), 890–902 (2006)
3. Bouchard, S., Gosselin, C., Moore, B.: On the ability of a cable-driven robot to generate a prescribed set of wrenches. *ASME Journal of Mechanisms and Robotics* **2**(1), 011,010 (2010)
4. Gosselin, C.: Cable-driven parallel mechanisms: State of the art and perspectives. *Journal of the Japan Society of Mechanical Engineers* **1**(1), 1–17 (2014)
5. Gouttefarde, M., Daney, D., Merlet, J.P.: Interval-analysis-based determination of the wrench-feasible workspace of parallel cable-driven robots. *Robotics, IEEE Transactions* **27**(1), 1–13 (2011)
6. Gouttefarde, M., Gosselin, C.: Analysis of the wrench-closure workspace of planar parallel cable-driven mechanisms. *Robotics, IEEE Transactions on* **22**(3), 434–445 (2006). DOI 10.1109/TRO.2006.870638
7. Guay, F., Cardou, P., Ruiz, A.L.C., Caro, S.: Measuring how well a structure supports varying external wrenches. In: 2nd Conference on Mechanisms, Transmissions and Applications. Bilbao, Spain (2013)
8. Merlet, J.P.: Analysis of the influence of wires interference on the workspace of wire robots. In: *Advances in Robot Kinematics*, pp. 211–218. Sestri Levante, Italy (2004)
9. Perreault, S., Cardou, P., Gosselin, C., Otis, M.: Geometric determination of the interference-free constant-orientation workspace of parallel cable-driven mechanisms. *ASME Journal of Mechanisms and Robotics* **2**(3), 031,016 (2010)
10. Pott, A., Meyer, C., Verl, A.: Large-scale assembly of solar power plants with parallel cable robots. In: 41st International Symposium on Robotics and 6th German Conference on Robotics, pp. 999–1004. Munich, Germany (2010)
11. Roberts, R.G., Graham, T., Lippitt, T.: On the inverse kinematics, statics, and fault tolerance of cable-suspended robots. *Journal of Robotic Systems* **15**(10), 581–597 (1998)
12. Stump, E., Kumar, V.: Workspaces of Cable-Actuated Parallel Manipulators. *Journal of Mechanical Design* **128** (2006). DOI 10.1115/1.2121741
13. Verhoeven, R.: Analysis of the workspace of tendon-based stewart platforms. Ph.D. thesis, Univ. Duisburg-Essen (2004)